

# Ultra Compact Objects in the Fornax Cluster of Galaxies: Globular clusters or dwarf galaxies?

Steffen Mieske<sup>1,2</sup>, Michael Hilker<sup>1</sup>, and Leopoldo Infante<sup>2</sup>

<sup>1</sup> Sternwarte der Universität Bonn, Auf dem Hügel 71, 53121 Bonn, Germany

<sup>2</sup> Departamento de Astronomía y Astrofísica, P. Universidad Católica, Casilla 306, Santiago 22, Chile

Received 30 October 2001 / Accepted 19 December 2001

**Abstract.** The relation between the Ultra Compact Objects (hereafter UCOs) recently discovered in the Fornax cluster (Drinkwater et al. 2000a, Hilker et al. 1999) and the brightest globular clusters associated with the central galaxy NGC 1399 has been investigated. The question was addressed whether the UCOs constitute a distinct population of objects not linked to globular clusters or whether there is a smooth transition between both populations.

Therefore, a spectroscopic survey on compact objects in the central region of the Fornax cluster was carried out with the 2.5m du Pont telescope (LCO). UCOs and the bright NGC 1399 globular clusters with similar brightness were inspected. 12 GCs from the bright end of the globular cluster luminosity function have been identified as Fornax members. Eight are new members, four were known as members from before. Their magnitude distribution supports a smooth transition between the faint UCOs and the bright globular clusters. There is no evidence for a magnitude gap between both populations. However, the brightest UCO clearly stands out, it is too bright and too large to be accounted for by globular clusters. For the only UCO included in our survey, a relatively high metallicity of  $[\frac{Fe}{H}] \simeq -0.5$  dex is measured.

**Key words.** galaxies: clusters: individual: Fornax cluster – galaxies: dwarf – galaxies: fundamental parameters – galaxies: luminosity function – globular clusters: luminosity function

## 1. Introduction

### 1.1. Magnitude - surface brightness relation of early type dwarf galaxies

The faint end of the galaxy luminosity function is mainly populated by dwarf elliptical galaxies (dEs) and dwarf spheroidals (dSphs, the faintest dEs in the Local Group). These galaxies are the most numerous type of galaxies in the nearby universe, having absolute magnitudes fainter than  $M_V \simeq -17$  mag. They follow a tight magnitude-surface brightness relation in the sense that central surface brightness increases with increasing luminosity (Ferguson & Sandage 1988, 1989). The validity of this relation has been a subject of lively debate over the last decade. A number of authors have argued against the existence of a magnitude-surface brightness relation for dEs (Davies et al. 1988, Phillipps et al. 1988, Irwin et al. 1990) and questioned the cluster membership assignment to dEs based on morphology.

Recently, spectroscopic membership confirmation has

shed light into this matter. Drinkwater et al. (2001a) do confirm the brightness - surface brightness relation for Fornax dwarfs based on the data of their Fornax Cluster Spectroscopic Survey (FCSS). They obtain spectra for all objects in the central 2 degrees of the Fornax cluster down to a limiting magnitude of  $M_V \sim -12.5$  mag and find that the magnitude surface brightness relation for dEs is well defined. Under this scheme, galaxies whose total luminosity and/or surface brightness lie significantly outside this relation are hard to classify. Two of the few examples for such peculiar objects that have been known for a long time are the high surface brightness compact dwarf elliptical (cdE) M32 and the very extended low surface brightness spiral Malin 1 (Bothun et al. 1987, Impey et al. 1988, Bothun et al. 1991).

### 1.2. New Ultra Compact Objects

Most recently, in the course of the FCSS, Drinkwater et al. (2000a) detected five ultra compact objects (UCOs, UCDs in their papers) within  $30'$  projected distance

Send offprint requests to: S. Mieske

Correspondence to: smieske@astro.uni-bonn.de

**Table 1.** Properties of the five UCOs. Adopted distance modulus to Fornax 31.3 mag. Magnitudes are from a photometric wide field survey of the central Fornax cluster (Hilker et al. 2002, in prep.). \* UCO 3 and 4 were detected first by Hilker et al. (1999).

Name	$\alpha$ (2000)	$\delta$ (2000)	$V$ [mag]	$M_V$ [mag]	$(V - I)$ [mag]	$r_{\text{eff}}$ [pc]	$d(\text{NGC 1399})$ [']
UCO 1	03:37:03.30	-35:38:04.6	19.31	-11.99	1.17	12	20.74
UCO 2	03:38:06.33	-35:28:58.8	19.23	-12.07	1.14	15	5.10
UCO 3*	03:38:54.10	-35:33:33.6	18.06	-13.24	1.20	50	8.26
UCO 4*	03:39:35.95	-35:28:24.5	19.12	-12.18	1.14	17	13.64
UCO 5	03:39:52.58	-35:04:24.1	19.50	-11.80	1.04	10	28.26

from the Fornax cluster’s central galaxy, NGC 1399<sup>1</sup>. Although as bright as average size dEs, they are by far more compact. Four of the five UCOs have absolute magnitudes of about  $M_V = -12$  mag, one is significantly brighter with  $M_V = -13.3$  mag. On HST-STIS images, the four fainter UCOs have King profile effective radii between 10 and 17 pc, while the brightest one has about 50 pc (Drinkwater et al. 2001b). In Table 1, the properties of the UCOs are summarized. All of them are significantly brighter than the brightest galactic globular cluster ( $\omega$  Centauri has  $M_V = -10.2$  mag) but significantly fainter than M 32 ( $M_V = -16$  mag). Neither Hilker et al. (1999), Drinkwater et al. (2000a, 2001b) nor Phillipps et al. (2001) could draw definite conclusions about the nature of the UCOs.

One possibility is that UCOs are bright globular clusters. NGC 1399 has a very rich globular cluster system with about 6000 GCs within  $10'$  (about 40 kpc at Fornax distance) from its center (Kohle et al. 1996, Forbes et al. 1998) which may contain GCs as bright as the UCOs. Another possibility is that UCOs are the nuclei of stripped dwarf galaxies. Threshing dE,Ns in the cluster potential has been shown to work (Bekki et al. 2001). Lotz et al. (2001) find that the luminosity function of 27 Fornax and Virgo dwarf nuclei peaks at  $V = 21.7$  mag ( $M_V = -9.6$  mag) with a dispersion of  $\sigma = 1.2$  mag, whereas the Globular Cluster Luminosity Function (GCLF) peaks at about  $M_V = -7.4$  mag. So, nuclei are on average more than 2 mag brighter than GCs and might mix up with the bright tail of the GCLF. Or do the UCOs represent a new group of ultra compact dwarf galaxies, extreme cases of M 32? No discriminating statement could be made until now.

It would be very interesting to know whether the UCOs had an origin different from the population of globular clusters of NGC 1399.

The UCOs have magnitudes roughly equal to the completeness magnitude limit of the FCSS ( $V = 19$  mag or  $M_V = -11.7$  mag). This is about 4.5 magnitudes brighter than the turnover of the globular cluster luminosity function (Kohle et al. 1996). In Fig. 1, the three relevant luminosity functions are shown in one plot: the LF of all observed sources in Drinkwater et al.’s FCSS (to

indicate its completeness limit); the LF of the UCOs; and the bright end of NGC 1399’s GCLF, represented by a Gaussian with  $V_{\text{to}} = 23.9$  mag and  $\sigma = 1.2$  mag, as taken from Kohle et al.’s GCLF. A total number of 8100 GCs was adopted, which is the number contained within  $20'$  from NGC 1399 (see Sect. 5.1.1).

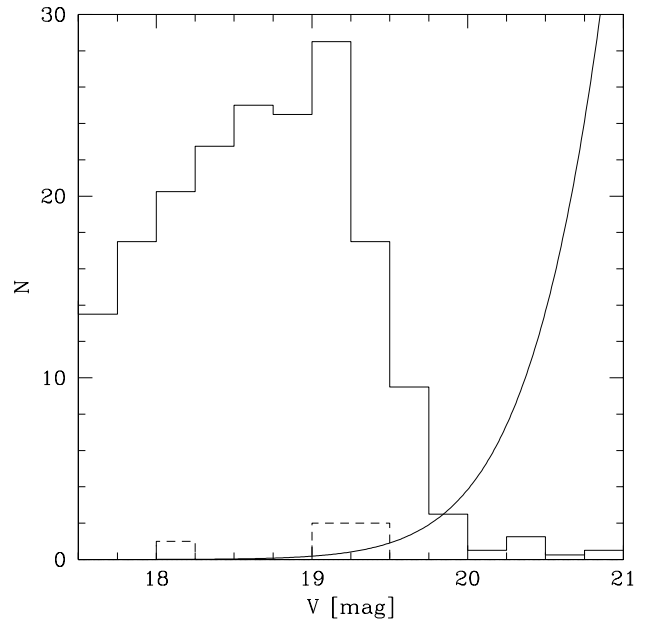


**Fig. 1.** *Solid line:* GCLF of NGC 1399, represented by a Gaussian with  $V_{\text{to}} = 23.9$  mag and  $\sigma = 1.2$  mag. Both values taken from Kohle et al. (1996). *Solid histogram:* LF of all observed sources in the FCSS in the central Fornax cluster, divided by four to fit into the plot (Drinkwater et al. 2001c,  $V$  magnitudes from Hilker et al. 2002, in prep.). It is shown to illustrate the FCSS’s completeness limit (90% at about  $V = 19$  mag). *Short dashed histogram:* LF of the UCOs.

### 1.3. Aim of this paper

As one can see in Fig. 1, the magnitude range between the UCOs and the bright globular clusters must be probed more thoroughly, both to know whether UCOs

<sup>1</sup> Two of them had already been detected by Hilker et al. (1999)

extend to fainter magnitudes and to determine the bright end of the GCLF. A gap in magnitude space between both populations would imply that the UCOs are very compact dEs or nuclei of stripped dwarfs rather than globular clusters.

In this paper, we describe and analyse a survey of compact objects in the central region of the Fornax cluster of galaxies that closes the magnitude gap between the FCSS and the globular cluster regime.

In Sect. 2 we describe the selection of candidates for the survey. In Sect. 3 the observations and data reduction are described. Sect. 4 shows the radial velocity measurement. In Sect. 5 the results are analyzed, the question whether or not the UCOs are a distinct population is discussed and metallicities of a number of Fornax dE,Ns are measured. These results are discussed in Sect. 6. Finally, in Sect. 7 a summary and conclusions are presented.

## 2. Selection of candidates

To choose candidates for our spectroscopic survey, we analyzed existing wide field images of the Fornax cluster. Those had been obtained over four nights in December of 1999 with the 2.5m Du Pont Telescope at Las Campanas Observatory, Chile. Their field of view was  $25' \times 25'$ ; 14 fields were observed. These fields map a circular region of 2 degrees diameter around the central giant elliptical galaxy, NGC 1399. The seeing ranged from  $1.5''$  to  $2''$ , which corresponds to a spatial resolution of  $\approx 120 - 160$  pc at the distance of the Fornax cluster, assumed to be 18 Mpc (Kohle et al. 1996). The pixel scale was  $0.774''/\text{pixel}$ . Images in  $V$  and  $I$  bandpasses were obtained for all fields. One of the central fields was also observed in  $B$ . Details of the photometry and of the calibrations will be presented in an accompanying paper (Hilker et al. 2002, in prep). All object magnitudes mentioned in this work are taken from that paper.

### 2.1. Unresolved objects

In turn, we describe the *compact* objects selection criteria for spectroscopy. These criteria are based on object brightness, colour and morphology.

The faint magnitude limit was set by analyzing the GCLF of NGC 1399, as determined by Kohle et al. (1996). They adopt a Gaussian distribution for the GCLF and estimate a turn over magnitude of  $V_{\text{to}}=23.9$  mag ( $M_V = -7.4$  mag) and a dispersion of  $\sigma=1.2$  mag. Since one of our goals was to include bright globular clusters (GCs), we defined  $V_{\text{faint}}=21$  mag as the faint magnitude limit for our observations, which is  $2.4 \sigma$  brighter than the turn over. This means that about 0.8% of all globular clusters around NGC 1399 would be accessible to our survey. Adopting 6000 as the total number (Kohle et al. 1996), then about 50 GCs would enter in our survey. The bright magnitude limit is given by the FCSS, which covers basically all ob-

jects down to  $V \approx 19$  mag.

Apart from pure brightness limits, other restrictions had to be made. Four of the five UCOs are unresolved on our CCD images due to their small diameter of about  $0.2''$  or 15 pc at Fornax distance (Drinkwater et al. 2001b). We did therefore not expect compact Fornax members in the magnitude regime fainter than the UCOs to be resolved on our images. Thus, unresolved sources were interesting in the first place. A source on our images was defined as unresolved, when SExtractor's star-classifier value (0 for a "perfect" galaxy, 1 for a "perfect" star, see Bertin & Arnouts 1996) was larger than 0.45 in both  $V$  and  $I$ . It was defined as resolved when this was not the case.

Of the unresolved objects in the mentioned magnitude regime, only those which had  $(V - I) < 1.5$  mag were accepted as candidates. The value 1.5 comes from the following consideration: we wanted to include all possible kinds of galactic nuclei or bright globular cluster type objects, but exclude background galaxies at high redshift or very red giants in the foreground. According to Worthey's (1994) stellar population models, for a very old population of 15 Gyrs with  $[\frac{Fe}{H}] = 0$  one gets  $(V - I)=1.33$  mag. Taking into account model uncertainties, photometric errors - which were smaller than 0.05 mag - and reddening by dust (Schlegel et al. (1998) found  $E(B-V) = 0.013$  towards Fornax),  $(V - I)=1.5$  mag was chosen as the red colour limit. To avoid missing very young star forming nuclei, no blue limit was applied.

Fig. 2 shows a colour magnitude diagram for one of the selected fields, with the selected candidates for the survey and the objects marked.

The only UCO included in our survey is UCO 2. The other ones lie outside the fields we covered (see Sect. 5).

### 2.2. Resolved objects

The only UCO resolved on our images (UCO 3) is about 1 mag brighter than the magnitude completeness limit of the FCSS. Yet, it cannot be ruled out a priori that there are compact, but resolved Fornax members fainter than the completeness limit of the FCSS. Therefore we selected in addition to the unresolved objects the smallest resolved sources in the same magnitude colour range like the unresolved objects. They were given lower priorities in the mask creation process than the unresolved ones.

Apart from compact objects, we included the dE,Ns cataloged in Fergusons's Fornax Cluster Catalog (FCC) (Ferguson 1989) that were bright enough and in the field we wanted to observe. This made it possible to compare the spectral properties of these nucleus-dominated spectra with those of the UCOs.

## 3. Observations and data reduction

The observations were performed in the three nights of 2000/12/30 to 2001/01/01 at the 2.5m Du Pont at Las

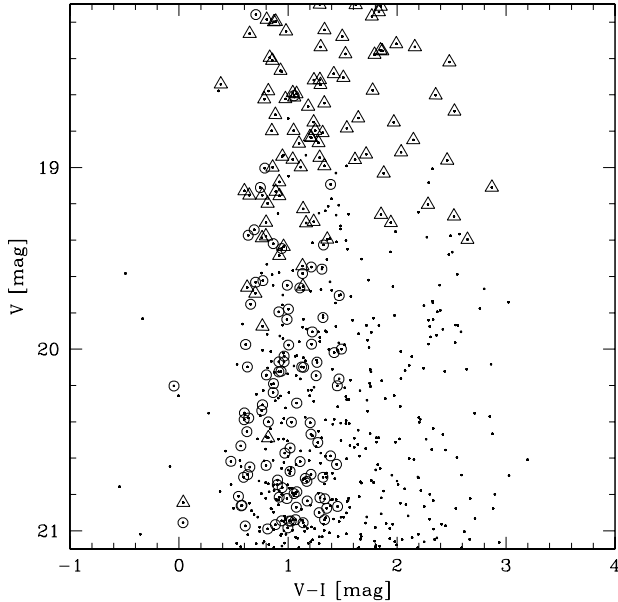


**Fig. 2.** Colour magnitude diagram of one of the selected fields, restricted to  $18.1 < V < 21.1$ . Points are all detected sources; open circles indicate sources satisfying our selection criteria for unresolved objects; open triangles are objects included in the FCSS (Drinkwater et al. 2000, private communication).

Campanas. The instrument was the Wide Field CCD (WFCCD) camera, which reimages a  $25'$  field onto a Tek#5-Detector of  $2048 \times 2048$  pixel with a pixel scale of  $0.774''/\text{pixel}$ . Multi-slit masks and the H & K grism, which has a good transmission between  $3500$  and  $6300 \text{ \AA}$  and a resolution of about  $1.3 \text{ \AA}$  per pixel, were used. As the slit width in our observation was  $\approx 1.5''$  ( $= 2$  pixel), the effective resolution was in the order of  $2.5 - 3 \text{ \AA}$ , corresponding to  $200 \text{ km/s}$  at  $4000 \text{ \AA}$ . Four fields were observed, with integration times of roughly  $3$  hrs each. In total we obtained spectra of  $160$  objects ( $40$  per field), of which about  $100$  were unresolved on our images.

All the data reduction was performed with the IRAF-packages IMRED and TWODSPEC. After bias subtraction, the cosmic rays were removed. The combined dome-flats were normalized to unity and the sky-flats were divided by the normalized dome-flats. The remaining illumination change along the slit was measured on these sky-flats. The single object exposures were then flat-field divided and corrected for the remaining illumination change. The object exposures were corrected for the tilting caused by the optics of the WFCCD camera and then combined. After these reduction steps, the spectra were extracted.

## 4. Radial velocity measurement

Radial velocities were determined by performing Fourier cross correlation between object and template spectra with the IRAF-task FXCOR.

### 4.1. Templates

As templates for the radial velocity measurement we used two of our standard star spectra (HD 54810 and HD 22879) and one synthetic spectrum taken from Quintana et al. (1996). These three templates showed the highest correlation peaks when cross correlating them with the four brightest Fornax dE,Ns included in our survey. When measuring the radial velocities with these templates, we accept the result as correct if the confidence level  $R$  (the  $r$ -ratio of Tonry & Davis 1979, defined as the relative height of the cross-correlation peak with respect to the neighbouring peaks) of the cross correlation peak between the template and the object spectrum is larger than  $3.5$  for all three templates. This corresponds to a S/N of about  $4$  between  $4500$  and  $5000 \text{ \AA}$ .

### 4.2. Results

In total we obtained  $164$  spectra in four fields. For  $40$  of those, the S/N was too low to reliably determine radial velocities. We successfully determined radial velocities for  $66$  foreground stars,  $18$  Fornax members and  $40$  background galaxies. Besides five dE,N candidates and UCO 2,  $12$  unresolved objects turned out to have a radial velocity between  $600$  and  $2500 \text{ km/s}$ , so they are probable Fornax members. We regard the unresolved objects as GC candidates (GCCs) from now on, since they are fainter than the UCOs. They are all within  $20'$  projected distance from NGC 1399. Eight of them have not been measured spectroscopically before, they are newly discovered members of the Fornax cluster. Two of the remaining four objects were known to be cluster members from Hilker (NTT 1998, private communication); the other two from Kissler-Patig et al. (1999). The five dE,Ns and UCO 2 can be confirmed as cluster members. The parameters of all Fornax members included in our survey are given in Table 2. The names of the dE,Ns are from the Fornax Cluster Catalogue (FCC) of Ferguson (1989). The names of our GC candidates are ‘‘FCOS Field Number–Object number’’. ‘‘FCOS’’ stands for ‘‘Fornax Compact Object Survey’’. The field number is:  $1$  for the south-east field,  $2$  for the south-west field and  $4$  for the north-west field, as shown in Fig. 3c). The object number is taken from the mask-creation file. The radial velocities, their errors and the confidence level  $R$  were computed by averaging the values given from FXCOR for each of the three templates. A list of all foreground and background sources is given in the Appendix. They are available electronically at <http://www.XXX>. As the highest object number is  $105$

**Table 2.** Fornax members, ordered by magnitude. See text for explanation of names.  $R$  is the confidence level of the cross correlation peak averaged over the three templates used. GCC stands for ‘‘Globular Cluster Candidate’’. In the comments-column, values for the radial velocities measured by other authors are given. The references are <sup>a</sup> Drinkwater (2000a), <sup>b</sup> Drinkwater and Gregg (1998), <sup>c</sup> Hilker et al. (1999), <sup>d</sup> Held and Mould (1994), <sup>e</sup> Drinkwater (2000, private communication), <sup>f</sup> Hilker (NTT 1998, private communication), <sup>g</sup> Kissler-Patig et al. (1999).

Name	$\alpha$ (2000.0)	$\delta$ (2000.0)	$v_{\text{rad}}[km/s]$	$R$	$V$	$(V - I)$	Type	Comment
FCC 222	3:39:13.23	-35:22:17.6	$825 \pm 25$	10.7	14.91	1.11	dE,N	$850 \pm 50^c$
FCC 207	3:38:19.42	-35:07:44.3	$1420 \pm 20$	20.3	15.34	1.03	dE,N	$1425 \pm 35^d$
FCC 211	3:38:21.65	-35:15:35.0	$2325 \pm 15$	31.0	15.65	1.04	dE,N	$2190 \pm 85^e$
FCC B1241	3:38:16.79	-35:30:27.0	$2115 \pm 25$	11.9	16.84	0.87	dE,N	$1997 \pm 78^b$
FCC 208	3:38:18.88	-35:31:50.8	$1720 \pm 50$	7.0	17.18	1.06	dE,N	$1694 \pm 84^c$
UCO 2	3:38:06.41	-35:28:58.2	$1245 \pm 15$	18.8	19.15	1.13	UCO	$1312 \pm 57^a$
FCOS 1-021	3:38:41.96	-35:33:12.9	$2010 \pm 40$	7.7	19.70	1.18	GCC	$1993 \pm 55^f$
FCOS 1-060	3:39:17.66	-35:25:30.0	$980 \pm 45$	8.2	20.19	1.27	GCC	
FCOS 1-063	3:38:56.14	-35:24:49.1	$645 \pm 45$	8.1	20.29	1.05	GCC	
FCOS 2-073	3:38:11.98	-35:39:56.9	$1300 \pm 45$	4.6	20.40	1.20	GCC	$v_{\text{rad}}=1300$ or 280
FCOS 1-019	3:38:54.59	-35:29:45.8	$1680 \pm 35$	5.6	20.62	1.01	GCC	$1730 \pm 80^f$
FCOS 1-058	3:38:39.30	-35:27:06.4	$1610 \pm 40$	5.8	20.67	1.04	GCC	$1540 \pm 150^g$
FCOS 2-078	3:37:41.83	-35:41:22.2	$1025 \pm 60$	4.6	20.69	1.21	GCC	
FCOS 2-086	3:37:46.77	-35:34:41.7	$1400 \pm 50$	5.74	20.81	0.92	GCC	
FCOS 4-049	3:37:43.09	-35:22:12.9	$1330 \pm 50$	5.0	20.85	0.98	GCC	
FCOS 2-089	3:38:14.02	-35:29:43.0	$1235 \pm 45$	8.21	20.87	1.08	GCC	
FCOS 2-095	3:37:46.55	-35:28:04.8	$1495 \pm 45$	3.9	20.96	1.14	GCC	$R < \text{limit}$ , $1186 \pm 150^g$
FCOS 1-064	3:38:49.77	-35:23:35.6	$900 \pm 85$	3.8	20.96	1.21	GCC	$R < \text{limit}$

(FCOS 2-105, a foreground star), one leading zero is used for originally two-digit numbers and two leading zeroes for originally one-digit numbers, such that all object numbers consist of three digits.

For three of the 12 GC candidates, namely FCOS 1-064, 2-095 and 2-073, the membership assignment is not definite. For objects 1-064 and 2-095, the confidence level  $R$  is lower than 3.5 for one of the templates, but larger for the other two. Cross correlation with all three templates yields the same (Fornax-) velocity within the error range. 2-073 has two cross correlation peaks at 1300 km/s and 280 km/s, both with  $R$  larger than 3.5 for all templates. The peak at 1300 km/s is 20% more pronounced than the peak at 280 km/s. Object 2-095 is one of the four objects that were known as Fornax members from before (Kissler-Patig et al. 1999). This indicates that our limits for  $R$  may be too strict. We therefore include all 12 GC candidates in our analysis.

## 5. Analysis

In this section a detailed analysis of the objects discovered is presented. From the total number of GCs associated with NGC 1399 (Dirsch et al. 2001, Forbes et al. 1998, Kohle et al. 1996), the form of its GCLF (Kohle et al. 1996) and the completeness of our survey we will calculate how many GCs should be included in our survey and compare that with the number we found. This will enable us to restrict the form of NGC 1399’s GCLF at the bright end. We also determine whether there is a statistically sig-

nificant gap in magnitude between the UCOs and our GC candidates. Lick line-indices are calculated for UCO 2 (see Table 2) and the dE,Ns included in our survey.

In Fig. 3a–d a colour magnitude diagram, a map of the loci of all successfully observed point sources, a colour velocity and a magnitude velocity diagram are shown. Note that in field 6, which is more than 1 degree away from the central galaxy NGC 1399, no GC candidates were found. In Fig. 4 the luminosity function for all our detections and for the GC candidates is given, including the 3 UCOs within 20’ from NGC 1399. The 2 UCOs outside 20’ that were included in Fig. 1 have been omitted in Fig. 4, because our area coverage outside 20’ is basically zero.

The mean radial velocity of the GC candidates is  $1300 \pm 109$  km/s with a standard deviation of  $\sigma=377$  km/s. Richtler et al. (2001, private communication), who obtained spectroscopy of about 350 GCs around NGC 1399, get  $1447 \pm 16$  km/s as the mean radial velocity. This is more than 1  $\sigma$  away from our result. However, we can rule out a systematic shift in our velocity values with respect to the measurements of other authors (see Table 2). For the ten objects with known radial velocities, the median of the difference between literature value and our value is  $-20$  km/s  $\pm 35$  km/s. With smaller samples biased to brighter GCs also other authors get smaller mean values: Minniti et al. (1998) found for a sample of 18 GCs around NGC 1399 a mean of  $1353 \pm 79$  km/s with  $\sigma=338$  km/s. Kissler-Patig et al. (1999) suggest with a larger sample of 74 GCs, that the velocity distribution of GCs around 1399 may even be bimodal with two peaks at 1200 and 1900 km/s, respectively.

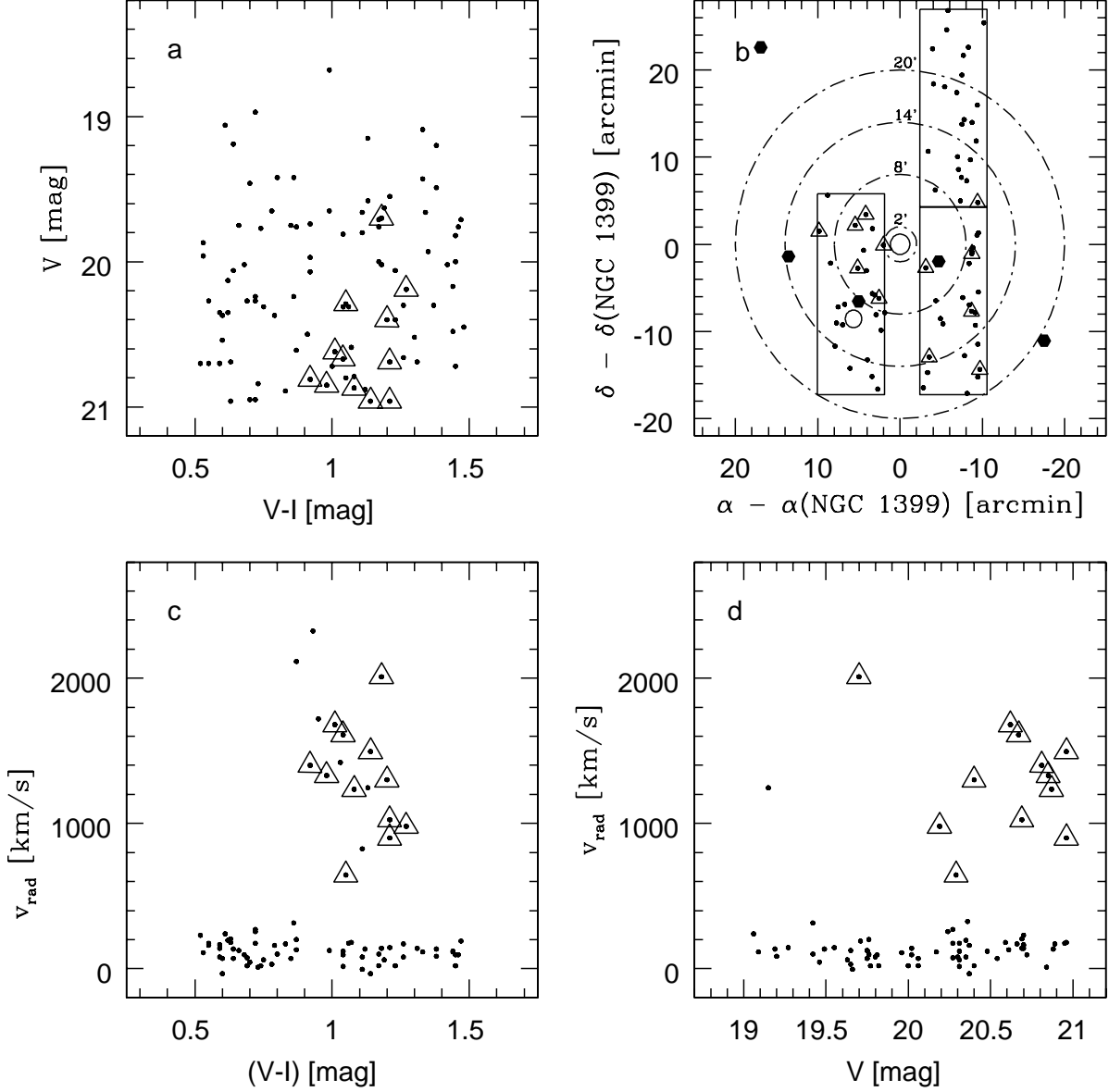


**Fig. 3.** Properties of successfully observed sources:

**a):** Colour magnitude diagram of the sources fainter than  $V = 18$  mag. **b):** Position diagram of the point sources centered around NGC 1399. NGC 1399 and NGC 1404 are indicated as open circles. Dot-dashed circles indicate distances of 2, 8, 14 and  $20'$  to 1399's center. The field limits are indicated as solid lines. For comparison, the positions of the UCOs are marked as filled hexagons. Only UCO 2 in the south west field was observed by us. **c):** Colour velocity diagram of all sources, except for background objects. Note that the 6 Fornax detections not marked with triangles are the 5 dE,Ns and UCO 2. GC candidates are marked as triangles. **d):** Magnitude velocity diagram of all sources, except for background objects and objects fainter than  $V = 18.7$  mag. Note that the dE,Ns are several magnitudes brighter than  $V = 18.7$  mag and are therefore not seen. The only Fornax member not marked with a triangle is UCO 2.

The colour magnitude diagram in Fig. 3a shows that the GC candidates have colours typical for GCs. Having a mean colour of  $(V - I) = 1.11$  with a standard deviation of 0.11, they are only slightly redder than the average  $(V - I) \simeq 1$  for GCs around NGC 1399.

Comparing the luminosity function of all unresolved objects in our survey with the GC candidates (see Fig. 4) shows that the latter ones are concentrated towards the faint end of our magnitude regime. Only one of the 12 GC candidates is brighter than  $V = 20$  mag, although we

cover the whole magnitude range between  $19 < V < 21$  mag ( $-10.3 < M_V < -12.3$  mag). This drop in frequency towards brighter magnitudes should be expected if all of the candidates are GCs. We are probing the regime 3 - 5 magnitudes brighter than the GCLF turnover magnitude ( $V_{\text{to}} \simeq -7.4$  mag) in which GC number counts should decrease towards brighter magnitudes. This is of course only a qualitative statement. To draw more quantitative conclusions, two questions need to be answered: can the number of our GC candidates be explained only by bright GCs belonging to NGC 1399's GCS? and, is there a significant magnitude gap between both populations? The next two subsections deal with these questions.

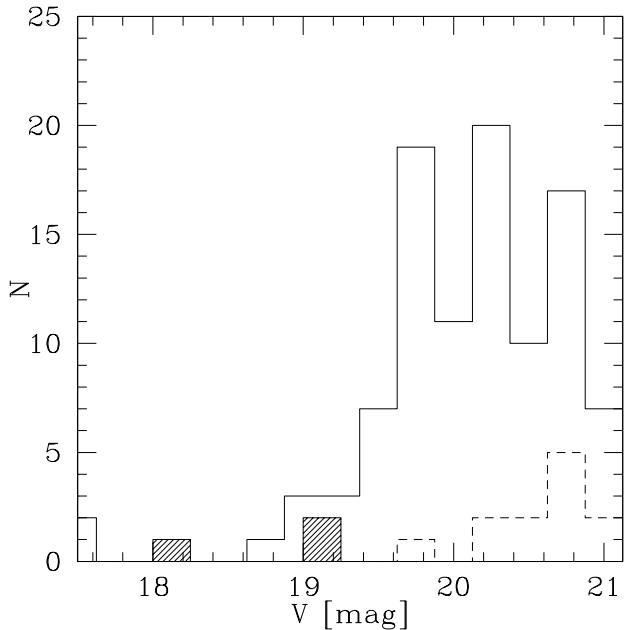


**Fig. 4.** *Solid histogram:* Luminosity function of all successfully observed unresolved objects. *Short dashed histogram:* Luminosity function of the GC candidates. *Shaded histogram:* Luminosity function of the UCOs within 20' of NGC 1399.

### 5.1. The expected number of globular clusters

How does the number of our GC candidates compare with the number expected from Kohle et al.'s (1996) GCLF? To find that out, three steps are necessary: First, the total number of GCs associated with NGC 1399 is calculated (Sect. 5.1.1). Second, the completeness of our survey is determined (Sections 5.1.2 and 5.1.3). Then the total number is multiplied with the completeness and the fraction of GCs brighter than our survey limit (Sect. 5.1.4). As the GC surface density and the completeness vary with radius, the calculations are performed separately for the three rings as shown in Fig. 3b.

#### 5.1.1. Total number of globular clusters associated with NGC 1399

Our detections reach out as far as almost 20' projected distance. Previous photometric studies of 1399's GCS, like those of Forbes et al. (1998) or Kohle et al. (1996), reached only 10'. To cover the zone between 10-20', the latest results of Dirsch et al. (2001) were used. Their data was obtained with the CTIO's MOSAIC camera and map the GCS of NGC 1399 out to a radius of 20'. At 20' they still find a GC surface density 2-3 times higher than in a comparison field 3.5 degrees away from the cluster center. Dirsch et al. subdivide the region around NGC 1399 into three rings with limits 0'-2.5', 2.5'-8' and 8'-20'. In Fig. 3b we adopted the ring limits equal to theirs (except for the innermost ring). There is a different slope in the radial density profile in all three rings. It holds in units of arcmin<sup>-2</sup>:

$$r \in [0; 2.5]' : \rho(r) = 10^{1.28} \quad (1)$$

$$r \in [2.5; 8]' : \rho(r) = 10^{0.98} \cdot r^{-0.77} + 10^{1.42} \cdot r^{-1.46} \quad (2)$$

$$r \in [8; 20]' : \rho(r) = 10^{1.46} \cdot r^{-1.41} + 10^{1.27} \cdot r^{-1.50} \quad (3)$$

The numbers of Dirsch et al. (2001) are not corrected for incompleteness. In order to estimate the fraction of objects missing, we integrated their number counts within 10', yielding  $1545 \pm 150$  GCs, and divided this by the total number of GCs within that region derived from previous surveys. We adopted the mean of the two values of Kohle et al. (1996) and Forbes et al. (1998), who get  $5940 \pm 570$  and  $5700 \pm 500$ , respectively. The ratio is then  $0.27 \pm 0.03$ .

With that information at hand, the number of GCs within each of the three rings, as plotted in Fig. 3b, is calculated by integrating the surface density law within the rings and dividing the numbers by 0.27. The GC candidate closest to NGC 1399 is only 2' away, so we integrated Dirsch et al.'s values from 2' to 8' instead of 2.5' to 8'. The results are:  $3800 \pm 460$  for ring 1 (2'-8'),  $2340 \pm 280$  for ring 2 (8'-14') and  $1960 \pm 230$  for ring 3 (14'-20').

#### 5.1.2. Photometric completeness

To determine the incompleteness involved in the source extraction on the photometric images, artificial star experiments were performed. With the IRAF task MKOBJECTS in the ARTDATA package 5000 artificial stars with Gaussian profiles were put into the V and I images of the three fields where the new members were found. Their magnitude ranged between  $21.5 > V > 19$  mag and their colour indices between  $2 > (V - I) > 0$  mag. Poisson noise was negligible compared to the stars' signal and was therefore not included. Magnitudes, colours and positions in the frame were randomly created using a C code.

To gain a statistically significant result without altering the crowding properties in our images, we added 50

**Table 3.** Total number  $N_{\text{sel}}$  and surface density  $n_{\text{sel}}$  of objects that satisfy our selection criteria and are in the central  $20'$  of the three fields where new members were found.

Field-Nr.	$N_{\text{sel}}$	$n_{\text{sel}}$ [arcmin $^{-2}$ ]
1	52	0.166
2	74	0.235
4	59	0.188
	$62 \pm 7$	$0.197 \pm 0.022$

times 100 artificial stars to our observed images. Then SExtractor was run on each of them, using the same parameters as on the original extraction. The photometric selection criteria for point sources as defined in Sect. 2 were then applied to the SExtractor output catalog.

The ratio between the number of artificial stars that match the selection criteria and the number of input artificial stars in that magnitude-colour-range defines the completeness in the photometric detection. For the objects in the magnitude-colour range of the selected candidates ( $19.5 < V < 21$  mag and  $0.4 < (V - I) < 1.5$  mag, see Fig. 2) the result is  $0.79 \pm 0.07$ . There is no significant magnitude dependence of the photometric completeness in the given magnitude regime. The differences between input and output magnitudes were on average smaller than 0.07 mag, with a standard deviation of  $\simeq 0.1$  mag. For all object magnitudes mentioned in this paper, the internal error is therefore on the order of 0.05 mag and for the colours it is about 0.07 mag.

### 5.1.3. Geometric completeness

The geometric completeness is obtained by dividing the surface density  $n_{\text{obs}}$  of successfully<sup>2</sup> observed point objects by the surface density  $n_{\text{sel}}$  of point objects that satisfy our selection criteria and were not included in the FCSS:

$$\text{Geometric completeness} = n_{\text{obs}}/n_{\text{sel}}.$$

$n_{\text{sel}}$  is distance independent. It was determined by counting the number  $N_{\text{sel}}$  of objects satisfying our selection criteria and not included in the FCSS in the central  $20'$  of the CCD frames of field 1, 2 and 4. The area covered is  $\pi * 10^2 = 314.2$  arcmin $^2$ , and therefore the resulting surface density is  $n_{\text{sel}} = \frac{N_{\text{sel}}}{314.2^2}$ . The numbers for both  $N_{\text{sel}}$  and  $n_{\text{sel}}$  are given in Table 3. The mean of  $n_{\text{sel}}$  is  $0.197 \pm 0.022$  arcmin $^{-2}$ .

To get  $n_{\text{obs}}$  for the three rings, we counted the number  $N_{\text{obs}}$  of point sources within each one and divided this value by the respective area:  $n_{\text{obs}} = \frac{N_{\text{obs}}}{\text{Area}}$ . These numbers, together with the magnitude independent geometric completeness  $\frac{n_{\text{obs}}}{n_{\text{sel}}}$ , are given in Table 4. Multiplying photometric and magnitude independent geometric completeness yields the total magnitude independent completeness  $C_0$  of our survey, ranging between 12 and 33%. The exact

<sup>2</sup> Here we implicitly treat the objects observed with too low S/N like the ones rejected for geometric reasons

**Table 4.** Surface density  $n_{\text{obs}}$  of observed unresolved objects in three rings around NGC 1399. The error of  $n_{\text{obs}}$  comes from the poisson error of  $N_{\text{obs}}$  which is its square root. The product of geometric ( $\frac{n_{\text{obs}}}{n_{\text{sel}}}$ ) and photometric (0.79) completeness, the total completeness  $C_0$ , is given in the last column.

Ring [ $''$ ]	$N_{\text{obs}}$	$n_{\text{obs}}$ [arcmin $^{-2}$ ]	$C_0 = \frac{n_{\text{obs}}}{n_{\text{sel}}} \cdot 0.79$
2-8	13	$0.069 \pm 0.023$	$0.28 \pm 0.08$
8-14	34	$0.082 \pm 0.014$	$0.33 \pm 0.07$
14-20	19	$0.030 \pm 0.007$	$0.12 \pm 0.03$
2-20	66	$0.053 \pm 0.007$	$0.21 \pm 0.04$

values for the three rings are summarized in Table 4.

Up to now, the magnitude dependence of the geometric completeness has not been considered; bright selected objects get higher priorities in the mask creation than faint ones, and the faint sources more likely have too low S/N. To take this into account, we subdivide the magnitude regime  $19 < V < 21$  in two bins of 1 mag width. For  $19 < V < 20$  mag the geometric completeness is  $1.18 \cdot C_0$ , for  $20 < V < 21$  mag it is  $0.92 \cdot C_0$ .

### 5.1.4. Observed number of Globular Clusters

As result of our radial velocity measurements we found 6 GC candidates inside ring 1, 5 in ring 2, and 1 in ring 3. If they are all GCs, the expected number of observed GCs should be close to these values for each ring.

In the last three subsections, the *existing* number of GCs in each of the three rings around NGC 1399, the photometric and the geometric completeness were calculated. The number of *expected* GCs is the number of existing ones multiplied by 0.8% (the bright end of the LF) and the total completeness. As only one of the 12 GC candidates is brighter than  $V = 20$  mag,  $0.92 \cdot C_0$  is adopted as the completeness (see Sect. 5.1.3). The results of these calculations are given in Table 5.

As one can see, the expected number of GCs matches well the number of GC candidates in all three rings.  $N_{\text{obs}}$  is always lower than  $N_{\text{exp}}$ , but the error ranges overlap. In other words, the radial distribution of our GC candidates agrees within the errors with the distribution of the whole GCS. Summing the values up, the total number of expected globulars is between 11 and 19 assuming a Gaussian LF with  $V_{\text{to}}=23.9$  mag and  $\sigma=1.2$ , when we observe 12. This is a good agreement, too. It implies that the bright tail of the GCLF is well described by a Gaussian and that the great majority of GC candidates really are GCs.

There are of course other representation for the GCLF. Kohle et al. (1996) fit a  $t_5$ -function to their data and find that the best value for  $\sigma$  is  $1.1 \pm 0.1$  mag, with the same turnover than for the Gaussian. Hilker et al. (1999) made estimates of the number of existing GCs in the bright



Ring [ $''$ ]	$N_{\text{exist}} \cdot 0.008$	$C_0 \cdot 0.92$	$N_{\text{exp}}$	$N_{\text{obs}}$
2-8	$30 \pm 6$	$0.253 \pm 0.082$	$7.6 \pm 2.8$	6
8-14	$19 \pm 4$	$0.305 \pm 0.074$	$5.8 \pm 2.4$	5
14-20	$16 \pm 4$	$0.112 \pm 0.040$	$1.8 \pm 1.4$	1
			$15.2 \pm 3.9$	12

**Table 5.** Number  $N_{\text{exp}}$  of expected GCs compared to the number  $N_{\text{obs}}$  of observed GC candidates. The errors of  $N_{\text{exist}} \cdot 0.008$  and  $N_{\text{exp}}$  are given by their square root.

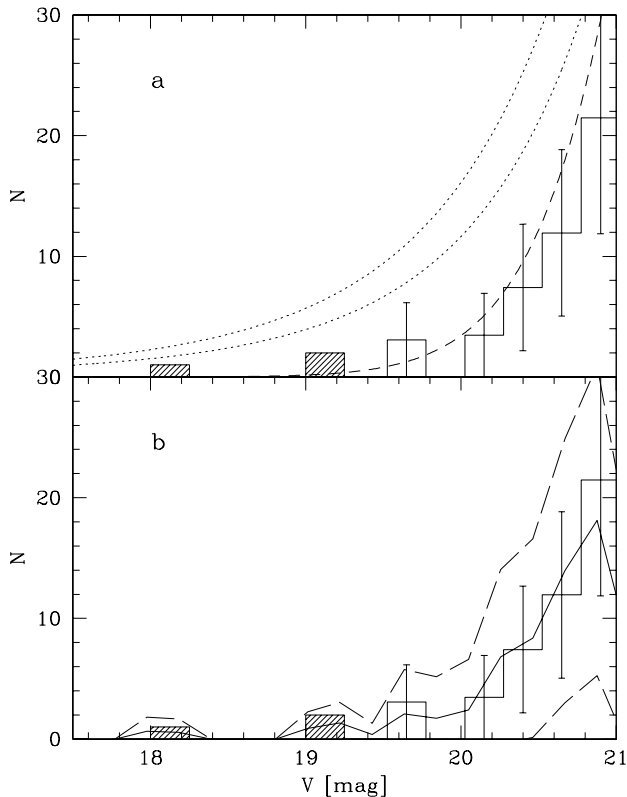


**Fig. 5. a):** *Solid histogram:* Incompleteness corrected LF of our GC candidates. Error bars are indicated. *Shaded histogram:* LF of the UCOs within  $20''$  of NGC 1399. *Dotted lines:*  $t_5$ -function with  $V_{t_0}=23.9$  mag,  $\sigma=1.1$  mag (upper line) and  $\sigma=1.0$  mag (lower line). *Short dashed line:* Gaussian with  $V_{t_0}=23.9$  mag and  $\sigma=1.2$  mag. Adopted total number of GCs: 8100 (see text). **b):** *Solid line:* Kernel estimator for the incompleteness corrected LF of our GC candidates, using an Epanechnikov kernel of width 0.125 mag. The error range is indicated by the long dashed curves. Histograms as in panel a).

manitude regime where they find 2 of the new UCOs ( $V=18.0$  and  $V=19.1$  mag, respectively). They adopt both a Gaussian and a  $t_5$ -function and find that GCs as bright as the brightest UCO can statistically only exist if the bright LF wings are described by a  $t_5$ -function. The fraction of GCs brighter than  $V=21$  mag, when adopting the  $t_5$ -function as in Kohle et al. becomes 2.3% (1.7% for

$\sigma=1.0$  mag). This is almost three times higher than for the Gaussian. The expected number of observed GCs in our survey would become  $44 \pm 8$ , by far higher than our result, even when including the UCOs as possible GCs. In Fig. 5a, the Gaussian ( $\sigma=1.2$  mag) and the  $t_5$  functions ( $\sigma=1.1$  and  $\sigma=1.0$  mag) are plotted together with the two luminosity functions. For the total number of GCs we adopt 8100, which is the sum of the values calculated for the three rings around NGC 1399 (see Sect. 5.1.1). The LF of our GC candidates is multiplied by the total completeness as determined in Sect. 5.1.3. Apparently, the LF is fit better by the adopted Gaussian than by the  $t_5$  functions, which significantly overestimate the number of bright GCs. The existence of GCs as bright as  $V = 18$  mag is therefore very unlikely.

## 5.2. A gap between the UCOs and our GC candidates?

From Fig. 5 one can see that the binning independent representation of the joint LF of GCs and UCOs is very well fit by the Gaussian. In the magnitude regime between 19.2 and 20.2 mag there is no evidence for a pronounced difference between the Gaussian and the data. We can therefore not confirm a significant gap in magnitude space between our newly found GC candidates and the 2 UCOs. There seems to be a smooth transition between both populations. This is consistent with the faint UCOs and the GC candidates belonging to the same group of objects, namely the brightest GCs of NGC 1399. However, the smooth transition observed by us is only a necessary and not a sufficient condition to link UCOs and GCs. Our data are consistent with a slight enhancement of number counts between  $V = 19$  and  $V = 20$  mag due to the presence of a small number of stripped nuclei, too (for further discussion, cf. Sect. 6).

## 5.3. Line indices and metallicities

### 5.3.1. Line indices

One of the UCOs (UCO 2) was included in our survey. In this section its line indices are compared with the observed Fornax dEs and the brightest GC candidate (object FCOS 1-021). The S/N of the other GC candidates is too low (4 - 6) to reliably measure line indices. In order to estimate metallicities and ages, we measured 8 line indices

as defined by Faber and Burstein (1973) and Brodie and Hanes (1986).

Brodie & Huchra (1990) determine a linear metallicity calibration for 7 of the 8 indices we used (not for Fe53), based on the Zinn & West (1984) scale for Galactic Globular Cluster metallicities:  $[\frac{Fe}{H}] = a \cdot I + b$ . Here,  $I$  is the line index,  $a$  and  $b$  are the coefficients of the linear calibration. To measure the line indices and their error for each of the confirmed Fornax members we followed closely the reduction procedure of Brodie & Huchra (1990). The object spectra were flux calibrated and all bandpasses were shifted according to the objects' radial velocity. The statistical error was determined from the original, not flux calibrated spectra.

In Fig. 6, the equivalent widths of  $H\beta$  (lower panel) and  $\langle Fe \rangle = (Fe52 + Fe53)/2$  (upper panel) are plotted vs. Mg2. The values for UCO 3 as determined by Hilker et al. (1999) are plotted as well. The red cutoff of object FCOS 1-021's spectrum is at about 5200 Å, therefore the measurement of Mg2 and  $\langle Fe \rangle$  is not possible for this object. For comparison, evolutionary tracks for different ages, taken from Worthey (1994) are overplotted. The metallicity range is  $-2 < [\frac{Fe}{H}] < 0.5$  dex for 17 and 8 Gyr and  $-1.7 < [\frac{Fe}{H}] < 0.5$  dex for 3 and 1.5 Gyr.

Of the 6 plotted objects, only FCC 207 and FCC 211 (both dE,Ns), have sufficiently high S/N to make a reliable age estimation. They appear to be quite old (age  $\geq 12$  Gyr) with metallicities between  $-1.0$  and  $-1.5$  dex according to Worthey's values. One can see that UCO 2 shows a high metallicity in comparison to the other objects (about  $-0.5$  in dex), but appears to be old as well, although error bars are large. The metallicity is calculated more accurately in the next section. UCO 3 (the brightest UCO, value from Hilker et al. 1999) appears very old, too. It is even more metal rich than UCO 2.

In the  $\langle Fe \rangle$  vs. Mg2 plot, five of our six objects and UCO 3 fall nicely into Worthey's evolutionary tracks, only FCC 222 apparently has a very high Fe abundance compared to the other objects.

### 5.3.2. Metallicities derived from line indices

We calculated the metallicity for each index (except Fe53) using the coefficients defined by Brodie and Huchra (1990) and then determined the weighted average  $[\frac{Fe}{H}]_w$  of the six different values.

The results for the seven Fornax members are given in Table 6. Only for UCO 2, FCC 207 and FCC 211 and FCC B1241 the weighted means have errors smaller than 0.5 dex. The metallicities of FCC 207 and FCC 211 lie well in the range of metallicities derived spectroscopically for bright Fornax dEs. Examples are Held & Mould (1994) ( $-0.75$  to  $-1.45$ ), Brodie & Huchra (1991) ( $-1.11 \pm 0.22$ ) or the most recent study from Rakos et al. (2001) ( $-0.4$  to  $-1.6$ ), the latter one based on Strömgren photometry. Held & Mould get  $[\frac{Fe}{H}] = -1.19 \pm 0.05$  for

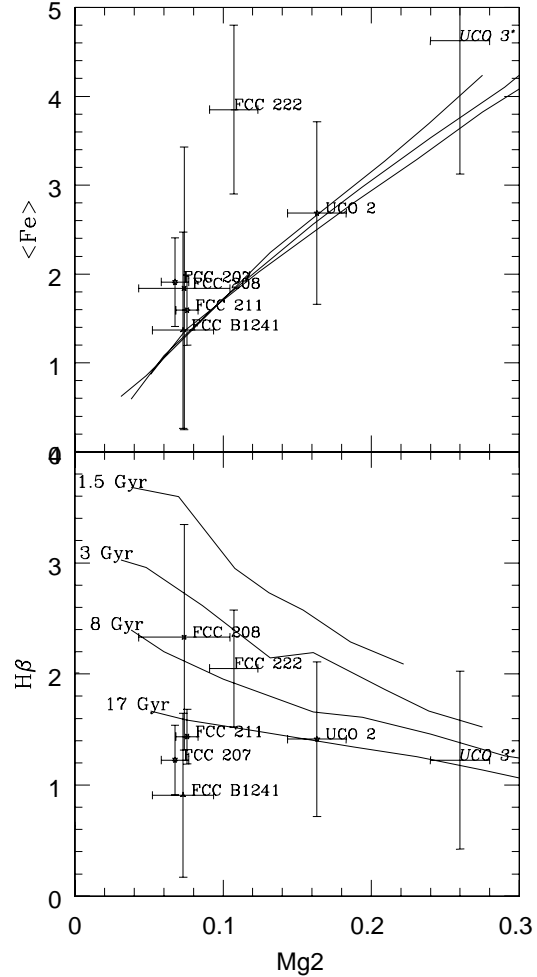


**Fig. 6.** *Upper panel:* Equivalent width of  $H\beta$  plotted vs. the line index Mg2. Evolutionary tracks for 1.5, 3, 8 and 17 Gyr as taken from Worthey (1994) are plotted as reference. Their metallicity range is  $-2$  ( $-1.7$  for 1.5 and 3 Gyr)  $< [\frac{Fe}{H}] < 0.5$  dex. *Lower panel:*  $\langle Fe \rangle$  plotted vs. Mg2. Evolutionary tracks for 3, 8 and 17 Gyr (Worthey 1994) are overplotted for reference.

\* Values for UCO 3 from Hilker et al. (1994)

FCC 207, Rakos et al. get  $-1.50$  for both FCC 207 and FCC 211 and obtain  $[\frac{Fe}{H}] = -0.9$  for FCC 222. Thus, our values are consistent with the findings of other groups.

UCO 2 is metal rich compared to average dE,Ns. For NGC 1399, the average GC metallicity is about  $-1.0 \pm 0.2$  dex (Brodie & Huchra 1991, Kissler-Patig et al. 1998), but the metallicity distribution is bimodal with peaks at about  $-1.5$  and  $-0.5$  dex (Kissler-Patig et al. 1998). Thus, UCO 2 is more metal rich than the mean, but could belong to the metal rich GC population. Hilker et al. (1999) find that UCO 3 is with  $[\frac{Fe}{H}] \simeq 0$  significantly metal richer than the dE,Ns, while UCO 4 shows similar line index values like the dE,Ns, however with very large errors.

Name	$[\frac{Fe}{H}]_w$ [dex]
UCO 2	$-0.57 \pm 0.28$
FCC B1241	$-1.41 \pm 0.37$
FCC 208	$-1.85 \pm 0.74$
FCC 207	$-1.34 \pm 0.41$
FCC 211	$-1.39 \pm 0.24$
FCOS 1-021	$-0.17 \pm 0.74$
FCC 222	$-0.74 \pm 0.68$

**Table 6.** Results for the weighted mean  $[\frac{Fe}{H}]_w$  derived from 6 different line indices (see text).

The most compact known dE M 32 is known to have a metallicity close to the solar one (e.g. del Burgo et al. 2001). Thus, the relatively high metallicities of UCO 2 and 3 may not be too surprising, if it is an intrinsic property of these very compact objects. The nucleus dominated spectrum of FCC 222 shows a high metallicity (with large error) as well, so UCO 2 and 3 could be nuclei of entirely stripped dE,Ns like FCC 222, too.

## 6. Discussion

What can we learn about the nature of the UCOs from our data?

The statistical arguments presented in Sect. 5.1 suggest that all our GC candidates can be accounted for by GCs and that there is no significant gap between our GC candidates and the fainter UCOs: the expected number of GCs detected in our survey ( $15 \pm 4$ ) is very close to the number of our GC candidates (12) when assuming a Gaussian LF for the GCS around NGC 1399. Adopting a LF with more extended wings like a  $t_5$ -function overestimates the number of bright globulars by far ( $44 \pm 8$ ). We therefore conclude that the luminosity function at the bright end is significantly better fit by a Gaussian than a  $t_5$ . This makes the existence of bright GCs with magnitudes like the *brightest* UCO ( $M_V = -13.2$  mag) very unlikely.

The *fainter* UCOs ( $M_V \simeq -12$  mag) do not appear as special as they were thought to be, considering the shape of the LF as shown in Fig. 5c. It is remarkable in this context that Minniti et al. (1998) already found two GC candidates with  $V = 19.6$  and  $V = 19.8$  mag ( $M_V = -11.7$  and  $-11.5$  mag) about  $5'$  away from NGC 1399 in a region not covered by us in this survey. This supports our conclusions that there exists no significant gap between GCs and faint UCOs and that our incompleteness corrections are in the right order. Including the 2 UCOs outside  $20'$  we have confirmed Fornax members at  $V$  magnitudes of 19.1, 19.2, 19.3, 19.5, 19.6, 19.7, 19.8, 20.2 and fainter. The distinction between both groups of objects based only on their different brightnesses might not be appropriate. The FCSS (Drinkwater 2000a) was not deep enough to detect the extension of the UCOs to fainter magnitudes. Therefore the detected UCOs seemed

to be a separate group of objects. Now we can state that the GCS of NGC 1399 is so rich that it probably contains GCs as bright as the four fainter UCOs. However, this does not exclude that some of them are isolated nuclei of dissolved dE,Ns.

To link the UCOs to GCs, they not only have to share the same magnitude space, but need to have a mean radial velocity and spatial distribution consistent with the GCS of NGC 1399. Both properties can only be determined very unprecisely for a sample of five objects. Nevertheless we remark that the UCOs' mean radial velocity of  $1530 \pm 110$  km/s (Drinkwater et al. 2000a) is consistent with that of the whole GCS ( $1447 \pm 16$  km/s, Richtler et al. 2001 private communication). Drinkwater et al. (2000a) find that the UCOs are significantly more concentrated towards the cluster center than the Fornax dE,Ns, but have a shallower distribution than the GCS as derived from previous surveys (Grillmair et al. 1994, Forbes et al. 1998). However, the latest results by Dirsch et al. (2001) show that the GCS of NGC 1399 does extend to well beyond  $20'$  projected distance from the galaxy's center. The distribution of our 12 GC candidates is consistent with that (cf. Section 5.1.4). Therefore even the furthest UCO at  $28.3'$  projected distance can still be a member of the GCS.

In the FCSS, Drinkwater et al. (2000a) found that for all the UCOs, cross correlation yielded higher confidence levels when using K-type stars as templates than younger F-type stars. We can confirm this result in so far as that cross correlation with HD 54810, a K star, gives higher  $R$  values than for HD 22879, an F star. For the nucleated dEs included in our survey it is vice versa. Thus, the integrated stellar type of UCO 2 appears to be more similar to those of GCs than to those of dE,Ns.

If nuclei of entirely stripped dwarf galaxies exist they would be expected to mix up with the bright GCs, because on average they are more than 2 mag brighter than GCs (cf. Introduction). The results obtained by us do not speak against the existence of these "naked" dwarf elliptical nuclei. Depending on the frequency of stripping, a certain fraction of the UCOs and the GC candidates observed by us, could be accounted for by stripped nuclei. We could be observing the sum of the bright tail of the GCLF and the nucleus-LF. Without thorough theoretical treatment of the frequency of entire stripping, this is very hard to quantify, although the nuclei are certainly less frequent than GCs. The number of dE,Ns in the central Fornax region is only in the order of a few dozen (as well in Virgo, see Lotz et al. 2001). The timescale for a total stripping is in the order of several Gyr (Bekki et al. 2001). So the number of stripped nuclei should be much smaller than the number of GCs, but due to their higher average brightness might become significant at bright magnitudes. A possible effect of the "naked nuclei" would be that the number counts at the very bright end ( $V \simeq 19.5$  mag) are enhanced with respect to the extrapolation of the GCLF from the magnitude range between  $V = 20$  and  $V = 21$  mag to fainter magnitudes.

With our limited statistical sample this cannot be traced. We have only probed about 25% of the area within 20' from NGC 1399. A much better coverage of the inner 20' and extension to a distance of 30' (where the remaining two UCOs at  $V \simeq 19.4$  mag are found) is needed to make more definite statements. Although our results together with Minniti et al.'s (1998) detections are indicative for an extension of NGC 1399's GCS to about  $M_V = -12$  mag, they have to be confirmed on a more profound statistical basis. Observing time to substantially increase the area coverage of our survey has been approved.

The brightest UCO (UCO 3) clearly stands out from the others. It is more than 1 mag brighter than the rest and based on our results it cannot be explained by the GCS. UCO 3 thus probably is galaxian, either the compact remnant of a once extended dE,N ("naked nucleus") or a cdE which was already "born" as compact as it is now, or a non nucleated dE changed by some tidal process to a more compact shape.

From the metallicity and morphology of the UCOs no conclusive statement can be made: our metallicity value for UCO 2 is quite high (about  $-0.55$  in dex), implying a metallicity higher than the majority of Fornax dE,Ns. Still, dE,Ns with similar metallicities have been found (Rakos et al. 2001). Of special interest is that M 32 – the most similar dwarf galaxy to the UCOs – has a very high metallicity, about solar (Burgos et al. 2001). As well, UCO 2 could belong to the metal rich GC population of NGC 1399 (Kissler-Patig et al. 1998). No discriminating statement can be made from metallicity, and due to the still too low S/N of the spectrum, a reliable age determination is not possible.

In our images, UCO 3 is the only one which is not classified as a stellar-like object according to the selection criteria given in Sect. 2. Its FWHM is  $2.3''$ , when the seeing was  $1.85''$ . This corresponds to a diameter of about 170 pc, by far larger than any GC found so far. But, the other UCOs are all unresolved, they have effective radii of about 15 pc (HST-STIS data published in Drinkwater et al. 2001b). None of the UCOs shows low surface brightness features in the outer part away from the central peak, although we can detect features down to  $\simeq 26.5$  mag/arcsec<sup>2</sup> in  $V$  (Hilker et al. 2002, in prep.). If the UCOs are remnants of dE,Ns, the stripping has been extremely efficient.

## 7. Summary and conclusions

In this paper, we presented a spectroscopic survey on compact objects in the central region of the Fornax cluster. The aim was to survey the magnitude regime framed by the newly discovered ultra compact objects (UCOs) in Fornax (Drinkwater et al. 2000a, Hilker et al. 1999) and the brightest GCs around NGC 1399. In the FCSS, performed by Drinkwater et al., the UCOs are at the faint magnitude limit of their survey. We wanted to know whether these detections constitute the bright

tail of a continuous luminosity distribution with a smooth transition into the GC regime or whether they are a separate population.

The velocity measurements (cf. Sect. 4) resulted in the discovery of 12 GC candidates in the magnitude range between  $19.70 < V < 20.95$  mag ( $-11.6 < M_V < -10.35$ ), located all within 20' from NGC 1399. For four of them, cluster membership was known before. Their mean colour is  $\langle V - I \rangle = 1.11 \pm 0.11$  mag and their mean radial velocity  $1300 \pm 109$  km/s with  $\sigma = 377$  km/s.

In the subsequent analysis of the discoveries (cf. Sect. 5), the following results were obtained:

1. The expected number of observed GCs originating from NGC 1399's GCS is  $15 \pm 4$ , in good agreement with the 12 objects found. To calculate the expected number we assumed a Gaussian LF with  $V_{to} = 23.9$  mag and  $\sigma = 1.2$  mag taken from Kohle et al. (1996), used the GC surface density from Dirsch et al. (2001) and took into account photometric and geometric incompleteness.
2. Assuming a more extended  $t_5$  distribution for the LF as adopted by Kohle et al. (1996), the expected number of observed GCs rises to  $44 \pm 8$ , which is more than three  $\sigma$  higher than the number of observed objects. This implies that the LF has no extended bright wings. Hilker et al. (1999) found that only by assuming such an extended LF the brightest UCO can be explained as a GC.
3. There is no significant gap in magnitude space between our GC candidates and the four fainter UCOs within 20' of NGC 1399. The GCS of NGC 1399 appears to extend to  $M_V \simeq -12$  mag.
4. The only UCO included in our survey is slightly better fit by early stellar types, in contrast to the dE,Ns.
5. The only UCO included in our survey has a relatively high metallicity compared to the dE,Ns, but is in the range of metal rich GCs or very compact dwarfs with almost solar metallicity like M 32.

Considering only point 5, we can neither rule out nor confirm that the UCOs are bright GCs. From points 1 to 4 we conclude: the four UCOs fainter than  $V = 19.1$  mag ( $M_V = -12.2$  mag) can be well explained by the bright tail of the GCLF of NGC 1399. However, the apparent overlap of the two LFs is not sufficient to exclude the existence of stripped nuclei of formerly extended dE,Ns mixing up with the bright GCs. The faint UCOs are probably no extremely faint examples of cdEs, but are the brightest members of their object class (GCs or stripped nuclei). UCO 3, however, is so bright and large, that it probably is not a GC. It remains the most puzzling object.

*Acknowledgements.* We thank our referee Michael Drinkwater for his useful comments which helped to improve the paper. SM acknowledges support by the Heinrich-Hertz-Stiftung of the Ministerium für Bildung und Wissenschaft des Landes Nordrhein-Westfalen. MH and LI acknowledge support through "Proyecto FONDECYT 3980032" and "8970009", respectively. LI thanks *Proyecto Puente PUC*, CONICYT and

Pontificia Universidad Católica de Chile for partial funding.

## References

- Bekki K., Couch W.J., Drinkwater M.J., 2001, *ApJ* 552L, 105
- Bertin E., Arnouts S., 1996, *A&AS* 117, 393
- Bothun G.D., Impey C.D., Malin D.F. Mould, J.R., 1987, *AJ* 94, 23
- Bothun G.D., Impey C.D., Malin D.F., 1991, *ApJ* 376, 404
- Brodie J.P., Hanes D.A., 1986, *ApJ* 300, 258
- Brodie J.P., Huchra J.P., 1990, *ApJ* 362, 503
- Brodie J.P., Huchra J.P., 1991, *ApJ* 379, 157
- Davies J.I., Phillipps S., Cawson M.G.M., Disney M.J., Kibblewhite, E.J., 1988, *MNRAS* 232, 239
- del Burgo C., Peletier R. F., Vazdekis A., Arribas S., Mediavilla, E., 2001, *MNRAS* 321, 227
- Dirsch B., Geisler D., Richtler T., Forte J.C., 2001, *IAU Symp.* 207, in press
- Drinkwater M.J., Gregg M.D., 1998, *MNRAS* 296, 15
- Drinkwater M.J., Jones J.B., Gregg M.D., Phillipps S., 2000a, *PASA* 17, 227
- Drinkwater M.J., Phillipps S., Jones J.B., et al., 2000b, *A&A* 355, 900
- Drinkwater M.J., Gregg M.D., Holman B.A., Brown M.J.I., 2001a, *MNRAS* 326, 1076
- Drinkwater M.J., Bekki K., Couch W.J., et al., 2001b, *astro-ph/0106375*
- Drinkwater M.J., Engel C., Phillipps S., Jones J.B., Meyer M.J., 2001c, *AAO Newsletter*, 97, 4 (*astro-ph/0106374*)
- Faber S.M., 1973, *ApJ* 179, 731
- Ferguson H.C., Sandage A., 1988, *AJ* 96, 1520
- Ferguson H.C., 1989, *AJ* 98, 367
- Ferguson H.C., Sandage A., 1989, *ApJ* 346, 53
- Forbes D.A., Grillmair C.J., Williger G.M., Elson R.A.W., Brodie J.P., 1998, *MNRAS* 293, 325
- Grillmair C.J., Freeman K.C., Bicknell G.V. et al., 1994, *ApJ* 422, L9
- Held E.V., Mould J.R., 1994, *AJ* 107, 1307
- Hilker M., Infante L., Vieira G., Kissler-Patig M., Richtler T., 1999, *A&AS* 134, 75
- Hilker M., Mieske S., Infante L., 2002, in preparation
- Impey C., Bothun G., Malin D., 1988, *ApJ* 330, 634
- Irwin M.J., Davies J.I., Disney M.J., Phillipps, S., 1990, *MNRAS* 245, 289
- Kissler-Patig M., Kohle S., Hilker M., et al., 1997, *A&A* 319, 470
- Kissler-Patig M., Brodie J.P., Schroder L.L., et al., 1998 *AJ* 115, 105
- Kissler-Patig M., Grillmair, C.J., Meylan G., et al., 1999, *AJ* 117, 1206
- Kohle S., Kissler-Patig M., Hilker M., et al., 1996, *A&A* 309, 39
- Lotz J.M., Telford R., Ferguson H.C., et al., 2001, *ApJ* 552, 572
- Minniti D., Kissler-Patig M., Goudfrooij P., Meylan G., 1998, *AJ* 115, 121
- Phillipps S., Davies J.I., Disney M.J., 1988, *MNRAS* 233, 485
- Phillipps S., Drinkwater M.J., Gregg M.D., Jones J.B., 2001, *ApJ* 560, 201
- Quintana H., Ramirez A., Way M.J., 1996, *AJ* 111, 603
- Rakos K., Schombert J., Maitzen H.M., Prugovecki S., Odell A., 2001, *AJ* 121, 1974
- Richtler T., Dirsch B., Geisler D., 2001, *IAU Symp.* 207, in press
- Schlegel D.J., Finkbeiner D.P., Davis M., 1998, *ApJ* 500, 525
- Tonry J., Davis M., 1979, *AJ* 84, 1511
- West M.J., Cote P., Jones C., Forman W., Marzke R.O., 1995, *ApJ* 453, L77
- Worthey G., 1994, *ApJS* 95, 107
- Zinn R., West M.J., 1984, *ApJS*, 55, 45Z

## Appendix A: Tables of all foreground stars and background galaxies

Table A.1 contains the parameters of all foreground stars and Table A.2 of all background galaxies for which a radial velocity was determined.

The name given in the first column consists of the acronym FCOS (Fornax Cluster Compact Survey) followed by a sequence number of the field and the object reference number used in the mask creation process. An asterix \* means that the object’s radial velocity could be determined only by identification of emission lines, because cross correlation yielded unreliable results. These were objects that show *one* strong emission line on top of a faint continuum. In all cases with stronger continuum and clearly identifiable absorption lines present (H&K), this emission line proved to be the redshifted OII line at restframe 3727.3 Å. Therefore, whenever the continuum was faint, we looked for absorption features close to the emission line and calculated their restframe wavelength assuming that the emission line was OII. If the wavelength were equal to important absorption lines around 3727 Å such as H8, H9 and H10, we accepted the assumption that the emission line was OII and determined the corresponding redshift. When no reliable identification was possible, no redshift determination was done.

The second and third column are the right ascension and declination for epoch 2000.

In the fourth column, the radial velocity with its error is given. Both values were computed by averaging the values given from FXCOR for each of the three templates used for cross correlation. In case of emission line objects with very faint continuum, the error was derived from the uncertainty of the emission line position. For the four quasars discovered, redshift instead of radial velocity is given.

In the fifth and sixth column, apparent magnitude  $V$  and colour ( $V - I$ ) are given. Both values are from Hilker et al. (2002, in prep.).

Table A.2 contains an additional comments-column. Here, ELO stands for “Emission Line Object”. Quasars were identified by their extremely broad emission line features.

**Table A.1.** Foreground stars.

Name	$\alpha$ (2000.0)	$\delta$ (2000.0)	$v_{\text{rad}}[km/s]$	$V$	$(V - I)$
FCOS 6-052	3:34:55.50	-35:03:59.6	230 $\pm$ 60	20.70	0.52
FCOS 6-042	3:34:57.65	-35:03:23.0	195 $\pm$ 45	20.35	0.62
FCOS 6-050	3:35:01.50	-35:07:54.0	170 $\pm$ 25	20.66	1.26
FCOS 6-043	3:35:03.10	-35:17:31.9	325 $\pm$ 75	20.36	-0.13
FCOS 6-047	3:35:03.87	-35:14:01.7	180 $\pm$ 25	20.59	1.07
FCOS 6-041	3:35:05.55	-35:10:10.6	120 $\pm$ 25	20.31	1.04
FCOS 6-029	3:35:07.03	-35:06:16.8	45 $\pm$ 25	19.46	0.70
FCOS 6-048	3:35:07.30	-34:58:13.1	130 $\pm$ 25	20.61	0.87
FCOS 6-038	3:35:09.32	-35:18:47.1	175 $\pm$ 35	20.27	0.55
FCOS 6-030	3:35:13.04	-35:04:46.3	135 $\pm$ 25	19.49	1.38
FCOS 6-034	3:35:13.99	-35:05:02.6	80 $\pm$ 15	19.80	1.11
FCOS 6-027	3:35:17.25	-35:20:20.8	240 $\pm$ 35	19.06	0.61
FCOS 6-051	3:35:18.31	-34:58:21.7	160 $\pm$ 35	20.70	0.55
FCOS 6-037	3:35:19.47	-34:59:37.2	115 $\pm$ 15	20.17	1.44
FCOS 6-039	3:35:22.54	-35:07:03.6	75 $\pm$ 15	20.27	0.69
FCOS 6-033	3:35:22.66	-35:06:34.3	95 $\pm$ 15	19.76	1.46
FCOS 6-056	3:35:24.22	-35:16:50.8	135 $\pm$ 25	20.88	1.12
FCOS 6-066	3:35:25.08	-35:21:46.2	-35 $\pm$ 15	16.45	1.14
FCOS 6-028	3:35:26.75	-35:16:35.8	85 $\pm$ 15	19.2	1.38
FCOS 6-036	3:35:32.04	-35:16:01.0	110 $\pm$ 25	19.96	0.53
FCOS 2-050	3:37:42.65	-35:25:41.4	190 $\pm$ 25	19.34	0.69
FCOS 2-080	3:37:42.98	-35:42:14.5	140 $\pm$ 45	20.70	0.59
FCOS 2-105	3:37:43.04	-35:38:28.6	135 $\pm$ 35	19.19	0.64
FCOS 2-059	3:37:43.49	-35:25:57.7	190 $\pm$ 35	19.71	1.47
FCOS 4-021	3:37:44.01	-35:15:09.3	95 $\pm$ 25	19.81	1.04
FCOS 2-051	3:37:45.96	-35:27:23.4	315 $\pm$ 35	19.42	0.86
FCOS 4-037	3:37:46.43	-35:13:01.4	20 $\pm$ 35	20.40	1.23
FCOS 4-033	3:37:47.42	-35:17:18.1	80 $\pm$ 25	20.30	1.26
FCOS 2-054	3:37:49.39	-35:44:07.5	145 $\pm$ 25	19.55	1.21
FCOS 4-043	3:37:49.66	-35:19:43.0	165 $\pm$ 70	20.7	0.59
FCOS 4-036	3:37:51.18	-35:12:42.3	-35 $\pm$ 60	20.37	0.60
FCOS 4-026	3:37:51.66	-35:05:19.3	95 $\pm$ 25	20.02	0.68
FCOS 2-057	3:37:52.02	-35:33:07.7	125 $\pm$ 15	19.65	0.99
FCOS 4-029	3:37:52.49	-35:07:34.3	70 $\pm$ 45	20.06	0.64
FCOS 4-031	3:37:53.43	-35:22:00.7	270 $\pm$ 50	20.27	0.72
FCOS 4-027	3:37:54.57	-35:18:25.4	140 $\pm$ 35	20.02	1.18
FCOS 4-020	3:37:55.11	-35:16:57.7	145 $\pm$ 85	19.27	0.07
FCOS 4-056	3:38:00.85	-35:00:10.1	100 $\pm$ 45	16.48	0.93
FCOS 4-022	3:38:01.58	-35:02:23.3	20 $\pm$ 25	19.82	1.45
FCOS 2-070	3:38:05.23	-35:35:31.8	20 $\pm$ 110	20.21	1.45
FCOS 2-058	3:38:08.05	-35:33:28.9	-5 $\pm$ 15	19.66	1.11
FCOS 4-041	3:38:08.40	-35:20:46.2	70 $\pm$ 15	20.54	0.60
FCOS 4-028	3:38:09.46	-35:08:35.5	20 $\pm$ 25	20.06	1.23
FCOS 4-035	3:38:10.01	-35:04:33.5	80 $\pm$ 45	20.35	0.59
FCOS 2-079	3:38:12.93	-35:41:44.2	205 $\pm$ 35	20.69	0.63
FCOS 2-060	3:38:15.50	-35:43:28.2	125 $\pm$ 25	19.75	0.66
FCOS 1-035	3:38:38.45	-35:34:51.4	30 $\pm$ 60	19.65	0.78
FCOS 1-028	3:38:40.67	-35:36:52.3	285 $\pm$ 30	19.86	1.17
FCOS 1-023	3:38:42.69	-35:43:37.7	160 $\pm$ 45	20.37	0.79
FCOS 1-033	3:38:43.67	-35:35:05.0	200 $\pm$ 35	19.76	0.87
FCOS 1-061	3:38:45.81	-35:25:12.6	170 $\pm$ 45	20.89	0.83
FCOS 1-047	3:38:45.91	-35:32:40.6	60 $\pm$ 45	20.31	0.75
FCOS 1-024	3:38:46.11	-35:42:11.4	70 $\pm$ 35	19.75	0.85
FCOS 1-073	3:38:48.85	-35:40:16.4	115 $\pm$ 15	19.09	1.33
FCOS 1-049	3:38:49.43	-35:30:01.8	10 $\pm$ 50	20.84	0.73
FCOS 1-057	3:38:51.15	-35:27:41.2	175 $\pm$ 50	20.95	0.72
FCOS 1-025	3:38:59.26	-35:41:14.4	140 $\pm$ 50	20.69	1.31
FCOS 1-043	3:39:02.39	-35:33:53.4	175 $\pm$ 25	20.31	1.06
FCOS 1-041	3:39:06.29	-35:34:11.4	100 $\pm$ 15	19.76	1.17
FCOS 1-030	3:39:07.31	-35:36:02.2	255 $\pm$ 45	20.24	0.72
FCOS 1-053	3:39:10.81	-35:29:09.7	120 $\pm$ 35	20.48	1.44
FCOS 1-066	3:39:12.55	-35:21:22.7	60 $\pm$ 35	19.63	1.19

**Table A.2.** Background galaxies

Name	$\alpha$ (2000.0)	$\delta$ (2000.0)	$v_{\text{rad}} [km/s]$	$V$	$(V - I)$	Comment
FCOS 6-023*	3:34:57.34	-35:12:24.0	$16830 \pm 85$	18.97	0.72	ELO
FCOS 6-032*	3:34:59.92	-35:11:41.6	$57820 \pm 130$	19.71	1.17	ELO
FCOS 6-057*	3:35:00.09	-35:09:25.3	$z=2.17$	20.95	0.70	Quasar
FCOS 6-005*	3:35:03.08	-35:20:53.4	$49220 \pm 105$	19.57	0.85	
FCOS 6-006*	3:35:03.29	-35:00:33.8	$94500 \pm 175$	19.69	0.76	
FCOS 6-001	3:35:06.61	-35:10:53.5	$61840 \pm 50$	19.24	1.41	
FCOS 6-045*	3:35:26.93	-34:59:51.0	$100900 \pm 85$	20.52	1.30	ELO
FCOS 6-031	3:35:31.62	-35:02:49.9	$56950 \pm 50$	19.66	1.34	
FCOS 4-040*	3:37:39.46	-35:01:34.8	$75515 \pm 85$	20.45	1.48	
FCOS 2-055*	3:37:42.69	-35:32:29.2	$71045 \pm 140$	19.58	1.13	ELO
FCOS 4-007*	3:37:43.02	-35:13:56.1	$82650 \pm 155$	20.27	1.44	
FCOS 4-023*	3:37:43.30	-35:11:02.1	$z=2.29$	19.87	0.53	Quasar
FCOS 2-052	3:37:44.46	-35:36:18.0	$48195 \pm 45$	19.43	1.33	
FCOS 2-084*	3:37:44.59	-35:34:50.9	$41635 \pm 85$	20.79	1.08	ELO
FCOS 4-001*	3:37:44.62	-35:18:32.6	$84230 \pm 175$	19.63	1.09	ELO
FCOS 4-006*	3:37:45.37	-35:00:22.2	$49950 \pm 140$	20.12	0.91	ELO
FCOS 4-016*	3:37:45.63	-35:03:35.4	$76910 \pm 210$	21.04	0.83	ELO
FCOS 2-001*	3:37:46.47	-35:24:11.4	$64460 \pm 105$	19.17	1.40	ELO
FCOS 2-065*	3:37:46.65	-35:27:50.0	$33960 \pm 120$	20.02	1.42	
FCOS 2-071*	3:37:48.12	-35:33:57.8	$41755 \pm 120$	20.24	0.86	ELO
FCOS 2-031*	3:37:48.21	-35:29:12.1	$64800 \pm 140$	20.50	0.91	ELO
FCOS 4-025*	3:37:48.69	-35:04:23.1	$z=2.57$	19.97	0.92	Quasar
FCOS 2-085*	3:37:50.94	-35:39:47.2	$95380 \pm 175$	20.80	1.05	
FCOS 4-044*	3:37:52.48	-35:13:13.6	$87600 \pm 140$	20.72	1.00	
FCOS 4-024	3:37:55.60	-35:09:36.1	$50165 \pm 50$	19.93	1.35	
FCOS 4-008*	3:37:55.70	-35:06:53.0	$92200 \pm 120$	20.31	1.24	
FCOS 2-008	3:37:59.86	-35:39:04.4	$61900 \pm 80$	19.68	1.40	
FCOS 4-010*	3:38:02.74	-35:01:19.2	$33350 \pm 140$	20.45	0.58	
FCOS 4-032*	3:38:02.79	-35:08:55.4	$73095 \pm 160$	20.30	1.37	ELO
FCOS 2-066*	3:38:03.76	-35:36:07.9	$48325 \pm 85$	20.07	0.92	ELO
FCOS 4-030*	3:38:12.67	-35:16:20.3	$z=2.53$	20.13	0.62	Quasar
FCOS 4-003*	3:38:21.76	-35:09:22.5	$50260 \pm 140$	19.77	1.03	
FCOS 1-011	3:38:31.12	-35:39:13.4	$33455 \pm 85$	18.08	1.14	ELO
FCOS 1-007	3:38:42.45	-35:30:50.2	$33215 \pm 50$	20.10	1.24	
FCOS 1-003*	3:38:49.09	-35:24:12.0	$87600 \pm 210$	19.79	1.11	ELO
FCOS 1-006*	3:38:49.14	-35:29:20.2	$82330 \pm 225$	19.63	0.93	ELO
FCOS 1-008*	3:38:56.91	-35:31:10.9	$128801 \pm 300$	21.02	0.98	ELO
FCOS 1-013*	3:39:02.64	-35:41:49.5	$88492 \pm 190$	20.68	0.85	ELO
FCOS 1-029*	3:39:03.63	-35:36:14.6	$55305 \pm 155$	19.74	0.92	ELO
FCOS 1-075	3:39:08.18	-35:38:41.3	$48075 \pm 85$	18.68	0.99	ELO